AIP Journal of Applied Physics

Characteristics of emission polarization in a -plane nanorods embedded with InGaN/GaN multiple quantum wells

J. C. Li, T. C. Lu, H. M. Huang, W. W. Chan, H. C. Kuo, and S. C. Wang

Citation: Journal of Applied Physics **108**, 063508 (2010); doi: 10.1063/1.3483239
View online: http://dx.doi.org/10.1063/1.3483239
View Table of Contents: http://scitation.aip.org/content/aip/journal/jap/108/6?ver=pdfcov
Published by the AIP Publishing

Articles you may be interested in

Cross-sectional sizes and emission wavelengths of regularly patterned GaN and core-shell InGaN/GaN quantum-well nanorod arrays
J. Appl. Phys. **113**, 054315 (2013); 10.1063/1.4790710

InGaN/GaN quantum well structures with greatly enhanced performance on a-plane GaN grown using self-organized nano-masks
Appl. Phys. Lett. **99**, 181907 (2011); 10.1063/1.3658803

Carrier localization in m -plane InGaN/GaN quantum wells probed by scanning near field optical spectroscopy
Appl. Phys. Lett. **97**, 151106 (2010); 10.1063/1.3502482

Optical characteristics of a -plane In Ga N Ga N multiple quantum wells with different well widths
Appl. Phys. Lett. **90**, 181122 (2007); 10.1063/1.2735935

Properties of nonpolar a -plane InGaNGaN multiple quantum wells grown on lateral epitaxially overgrown a -plane GaN
Appl. Phys. Lett. **86**, 031901 (2005); 10.1063/1.1851007

Re-register for Table of Content Alerts

Create a profile.

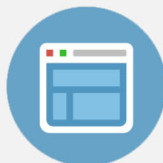

Sign up today!

[This article is copyrighted as indicated in the article. Reuse of AIP content is subject to the terms at: http://scitation.aip.org/termsconditions. Downloaded to] IP: 140.113.38.11 On: Wed, 30 Apr 2014 10:00:39

Characteristics of emission polarization in *a*-plane nanorods embedded with InGaN/GaN multiple quantum wells

J. C. Li, T. C. Lu,[a] H. M. Huang, W. W. Chan, H. C. Kuo, and S. C. Wang
Department of Photonics, National Chiao Tung University, 1001 University Road, Hsinchu 30010, Taiwan

(Received 26 January 2010; accepted 27 July 2010; published online 17 September 2010)

Nonpolar (*a*-plane) GaN nanorod arrays with embedded $In_xGa_{1-x}N/GaN$ (x=0.09, 0.14, 0.24, and 0.30) multiple quantum wells (MQWs) grown on *r*-plane sapphire have been fabricated successfully by self-assembled Ni nanomasks and subsequent inductively coupled plasma reactive-ion etching. After nanorod fabrications, the polarization ratio of the emission from MQWs with lower indium composition (x=0.09 and 0.14) slightly decreases but apparently increases by at most 79% for the samples with higher indium composition (x=0.24 and 0.30). Competition between the effect of multiple scattering, strain relaxation and reduction in localized centers, expected in *a*-plane MQW samples, are attributed to the variations in the polarization ratios after the nanorod formation. © *2010 American Institute of Physics*. [doi:10.1063/1.3483239]

I. INTRODUCTION

GaN-based devices have attracted much attention for optoelectronic applications like laser diode and light emitting diode (LED) (Ref. 1) due to their wide direct band gap with emission wavelength ranging from infrared to ultraviolet light. However, conventional *c*-plane multiple quantum well (MQW) structures suffer from the quantum confinement Stark effect due to the existence of strong piezoelectric and spontaneous polarization.[2,3] The built-in electric fields along *c*-direction cause spatial separation of electron and hole wave functions that in turn gives rise to the restriction of carrier recombination efficiency, the reduction in oscillator strength, which reduces the overall emission efficiency and the redshift in peak emission.[4] Recently, a promising method to eliminate the internal field is to grow InGaN/GaN MQWs on nonpolar orientations such as $\{11\bar{2}0\}$ *a*-plane GaN on $\{10\bar{1}2\}$, *r*-plane sapphire and *a*-plane SiC, and {10–10} *m*-plane GaN on {100} $LiAlO_2$ substrates.[5,6] In particular, due to the anisotropic in-plane compressive strain in nonpolar GaN-based materials, the original $|X \pm iY\rangle$-like valence-band states are broken into $|X\rangle$-like and $|Y\rangle$-like ones.[7] Therefore, an inherently polarized light will be emitted from InGaN/GaN MQWs grown on nonpolar GaN, which is intriguing for applications needing a polarized light source, such as liquid crystal display backlight modules.[8] Theoretical studies predict that the polarization ratio increases as indium composition increases.[9] However, it is well known that the low miscibility of InN in GaN leads to a large fluctuations of indium or phase segregation within InGaN layers,[10,11] which is believed to confine more carriers at localization centers and then reduce the polarization ratio.[12] As a result, the polarization ratio does not increase with the indium composition due to the enhancement of dotlike In-rich regions.[13] In this paper, we report a viable method to improve the polarization ratio of *a*-plane InGaN/GaN MQWs with higher indium composition using nanorod-fabrication technique. In addition, the optical properties of *a*-plane GaN nanorod arrays with embedded InGaN/GaN MQWs on *r*-plane sapphire were investigated to understand the origin of the variations in the polarization ratio after nanorod fabrication.

II. EXPERIMENT

Four *a*-plane $In_xGa_{1-x}N/GaN$ MQWs with different indium compositions were grown on *r*-plane sapphire with 0.2 offcut by metal organic chemical vapor deposition reactor. Trimethylgallium, trimethylindium, and ammonia were the precursors used as sources of Ga, In, and N in the whole epitaxial process. The *a*-plane $In_xGa_{1-x}N/GaN$ MQWs structures consisted of a 30-nm-thick AlN nucleation layer, 2-μm-thick bulk GaN, 1-μm-thick *n*-type GaN, ten pairs of MQWs with 18-nm-thick GaN barrier, 4.5-nm-thick InGaN well and finally a 50-nm-thick GaN capping layer. The detailed growth parameters were reported elsewhere.[14] The x-ray diffraction analysis confirmed that the indium compositions in the QWs were around 0.09, 0.14, 0.24, and 0.30 for the four samples, respectively. The grown *a*-plane MQWs were then subjected to the nanorod manufacturing process as shown in Fig. 1(a). First, a thin layer of Ni metal about 10 nm was deposited on the surface by E-gun evaporator. The Ni-coated *a*-plane MQWs samples were subsequently subjected to rapid temperature annealing under flowing N_2 at 850 °C for 1 min to form self-assembled Ni metal clusters. Then, the *a*-plane MQWs samples were etched down to the *n*-type GaN layer by the inductively coupled plasma reactive-ion etching (ICP-RIE) system (SAMCO ICP-RIE 101iPH) operated at 13.56 MHz under a gas mixture of $Cl_2/Ar=45/30$ SCCM (SCCM denotes cubic centimeter per minute at STP) with 2 min of etching time to form nanorods. The ICP source power, bias power, and the chamber pressure of the ICP-RIE system were set at 400/40 W. Finally, the samples were dipped into a heated nitric acid solution (HNO_3) at 100 °C for 5 min to remove the residual Ni nanomask. Figure 1(b) shows the birds-view (left) and cross-sectional (right) field-emission scanning electron microscopy (FESEM) image of the fabricated *a*-plane InGaN/GaN

[a]Electronic mail: timtclu@mail.nctu.edu.tw.

 © 2010 American Institute of Physics

[This article is copyrighted as indicated in the article. Reuse of AIP content is subject to the terms at: http://scitation.aip.org/termsconditions. Downloaded to] IP: 140.113.38.11 On: Wed, 30 Apr 2014 10:00:39

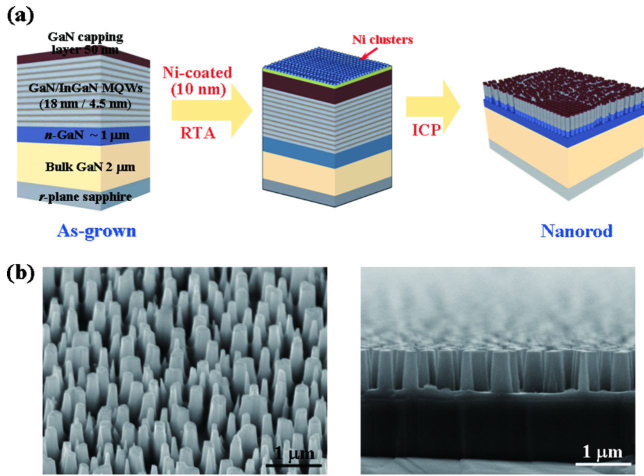

FIG. 1. (Color online) (a) The schematic of the a-plane InGaN/GaN MQWs nanorod-fabrication process. (b) The birds-view (left) and cross-sectional (right) FESEM image of the fabricated a-plane InGaN/GaN MQW nanorods. The density, diameter and heights of the nanorods were and 1×10^9 cm^{-2}, 250 nm, and 0.6 μm, respectively.

MQWs nanorods. The dimension and density of the fabricated nanorods were estimated from the SEM image to be 250 nm and 1×10^9 cm^{-2}, respectively. The etching depth estimated from the image is about 0.6 μm.

For the polarization-dependent photoluminescence (PL) measurements, the samples were excited by a 325 nm HeCd laser with an excitation power of 35 mW and the emitted luminescence light was collected using a polarizer in front of the spectrometer (Triax 320) with a charge-coupled device detector. By rotating the polarizer, we could collect the light with electrical field perpendicular ($E\perp c$) and parallel ($E\parallel c$) to the c-axis, respectively. The focused spot size of the HeCd laser was estimated to be about 200 μm in diameter. In addition, temperature-dependent PL measurements were performed at temperatures ranging from 20 to 300 K.

III. RESULTS AND DISCUSSIONS

Figure 2 shows the integrated PL intensity of all samples after nanorod fabrication at different polarization angles at room temperature. It can obviously be seen that the PL intensity for all four samples increases with increasing polarization angle from 0° ($E\parallel c$) to 90° ($E\perp c$), implying that polarized light has been emitted from the a-plane InGaN/GaN MQWs nanorods. Moreover, since the spectral broadening is too large (about 200 meV), observable peak shift cannot be found between the emissions polarized to $E\parallel c$ and to $E\perp c$. The polarization ratios (ρ) for all samples are cal-

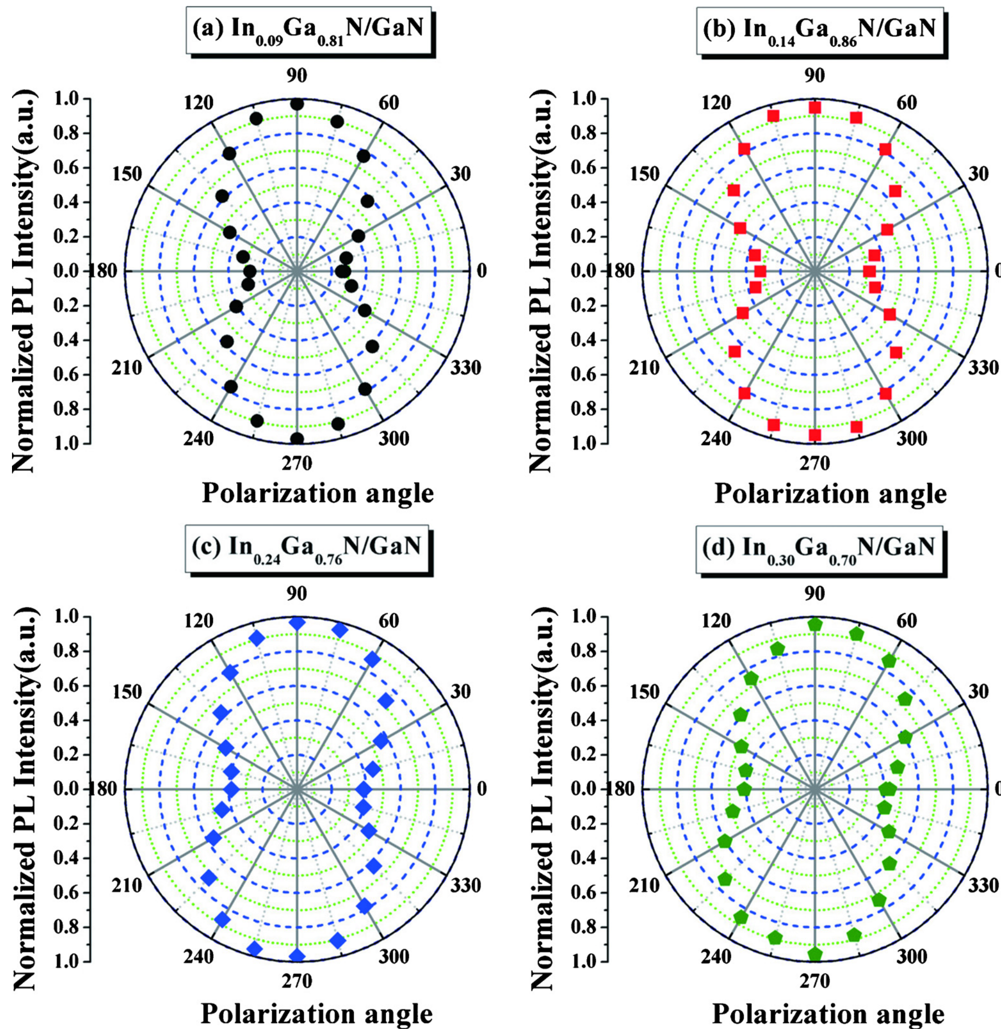

FIG. 2. (Color online) The integrated PL intensity of nanorod samples with indium composition of (a) 0.09, (b) 0.14, (c) 0.24, and (d) 0.30 at different polarization angles at room temperature.

[This article is copyrighted as indicated in the article. Reuse of AIP content is subject to the terms at: http://scitation.aip.org/termsconditions. Downloaded to] IP: 140.113.38.11 On: Wed, 30 Apr 2014 10:00:39

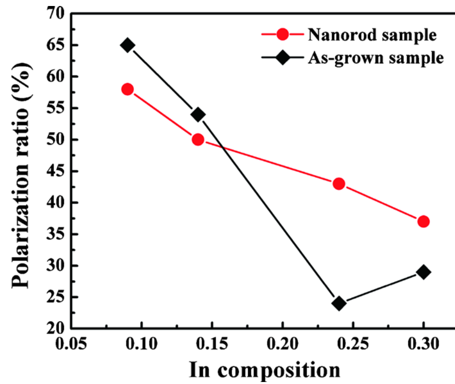

FIG. 3. (Color online) The polarization ratio plotted as the function of indium compositions for the as-grown and nanorod samples.

culated and summarized in Fig. 3, where ρ is defined as $(I_{\perp}-I_{\parallel})/(I_{\perp}+I_{\parallel})$ using the integrated PL intensity, I. At first glance, the polarization ratio ρ still decreases as indium composition increases. Interestingly, it is found that, as compared to the as-grown samples, the values of ρ decreases slightly by 11% and 7% in the nanorod samples with $x=0.09$ and 0.14, respectively, while it increases significantly by 79% and 27% in the nanorod samples with $x=0.24$ and 0.30, respectively. Previous structural and optical studies on the *c*-plane InGaN/GaN MQWs nanorods showed that the internal strain had been greatly reduced.[15,16] Accordingly, the anisotropy strains in the *a*-plane InGaN/GaN MQWs nanorods should also be released. Once the strain is decreased, subband-energy separation should be smaller,[17,18] which will lead to the reduction in the polarization ratio. In addition, multiple scattering should occur after the nanorod formation, which also can reduce the polarization ratio. However, considering the anomalous enhancement of ρ in the higher indium composition samples after nanorod fabrication, one can expect that there must be other mechanisms accounting for this phenomenon. In the following, further optical studies and discussions are carried out.

The temperature-dependent PL spectra of all samples were measured between 20 and 300 K with 20 K interval. The results for the sample with indium composition of 0.09 are displayed in Fig. 4. Similar to the as-grown samples, the spectra of the nanorod samples exhibit lower-energy (P_L) and higher-energy (P_H) emission peaks in the low-temperature range, which are attributed to the emissions from localized states and QWs, respectively. Nevertheless, it is noteworthy that both P_L and P_H peaks blueshift slightly after nanorod fabrication, and the P_H peak becomes dominant at low temperature. These behaviors can also be investigated in other nanorod samples. Generally, the dangling bonds, Ga/In or N vacancy, and other defects will be induced on the surface of the nanorods sidewalls during the ICP-RIE etching, which will lead to high densities of surface states. Therefore, the surface Fermi-level might enter into the conduction band, resulting in broadening of the optical band gap due to the Burstein–Moss effect.[19,20] Accordingly, the blueshifts for the P_L and P_H peaks are reasonable. In addition, such surface states may decrease the recombination rate of QWs near to the surface of side walls. This damage can be alleviated by optimizing the etching parameters or using the passivation approach.[21,22] What we concern here is the change in the integrated intensity ratio of the P_L to P_H peaks (denoted as P_L/P_H) after nanorod fabrication. Figure 5 shows the P_L/P_H at 20 K for all samples before and after nanorod fabrication. An apparent reduction in P_L/P_H can be observed in all samples, and it is decreased by 35%, 60%, 65%, and 49% for nanorod samples with $x=0.09$, 0.14, 0.24, and 0.3, respectively. This result suggests that the energy depth of localized states may have been reduced after nanorod fabrication. Thus more carriers would be confined in the quantized level of QW rather than in localized centers. Moreover, these shallower localized states may be another reason for the blueshift in the P_L peaks.

Furthermore, it has been studied that thermal quenching of PL intensity as temperature is increased can be explained by the thermal emission of the carriers out of a confining potential with the activation energy.[23] Therefore, it is expected that the shallower localized centers should have

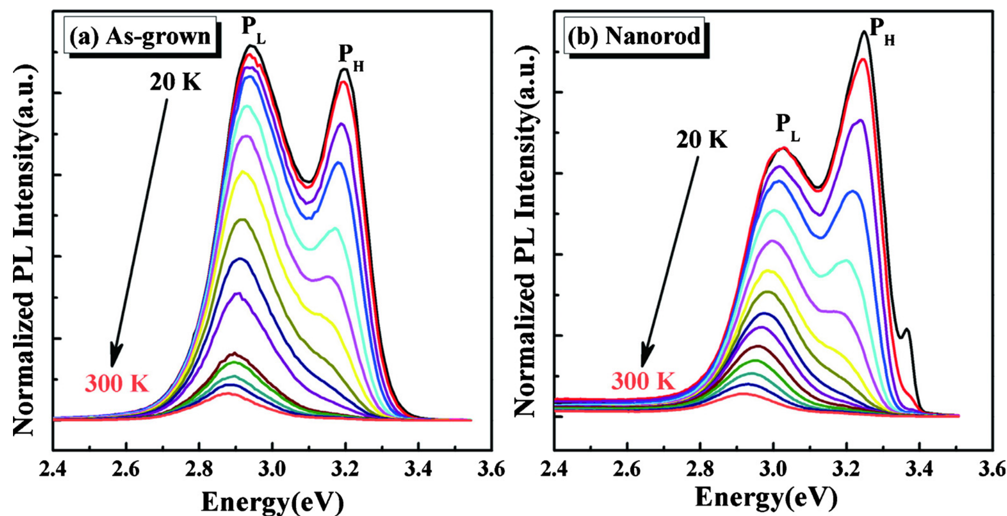

FIG. 4. (Color online) The temperature-dependent PL spectra for the (a) as-grown and (b) nanorod samples with indium composition of 0.09. The temperature increases from 20 to 300 K with 20 K interval.

[This article is copyrighted as indicated in the article. Reuse of AIP content is subject to the terms at: http://scitation.aip.org/termsconditions. Downloaded to] IP: 140.113.38.11 On: Wed, 30 Apr 2014 10:00:39

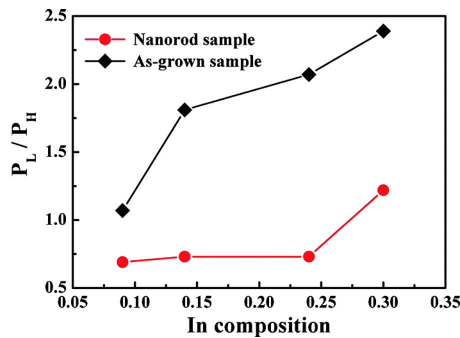

FIG. 5. (Color online) The integrated intensity ratio of the P_L to P_H peaks plotted as the function of indium compositions for the as-grown and nanorod samples measured at 20 K.

smaller activation energies. In order to verify that, the temperature dependence of PL intensity for all nanorod samples was fitted to an Arrhenius equation:

$$I(T) = \frac{I_0}{1 + A \exp\left(\frac{-E_a}{k_B T}\right) + B \exp\left(\frac{-E_b}{k_B T}\right)}, \quad (1)$$

where T is the temperature, I_T and I_0 are the integrated PL intensity for T and 0 K, A and B are constants, k_B is the Boltzmann constant, E_a is the activation energy for PL quenching, and E_b is generally associated to the free exciton binding energy.[23] The fitted activation energies E_a are listed in Table I. Compared to the as-grown samples, the value of E_a is indeed smaller, as expected. Particularly, the largest variation in E_a (about 16 meV) appears in the sample with indium composition of 0.24, which is consistent with the greatest reduction in the integrated intensity ratio of the P_L to P_H peaks mentioned above.

Based on these results, the variations in the polarization ratio observed in our nanorod samples can be explained as follows. By fabricating the nanorod structures, multiple scattering along with strain relaxation and reduction in localized centers occur in all samples, which are believed to decrease and increase the polarization ratio of the emission, respectively. In the case of the lower indium composition samples, the multiple scattering and strain relaxation is considered to be much stronger. While as the indium composition is continuously increased, the polarization ratio enhancement effect by the reduction in localized centers becomes dominant. Consequently, slight reduction and evident enhancement of the polarization ratio are observed in our *a*-plane nanorod samples with lower and higher indium compositions, respectively. In addition, the energy depth of localized centers in the sample with indium composition of 0.24 was found to be reduced more significantly than that in the sample with indium composition of 0.30, resulting in much stronger enhancement effect for polarization ratio. Thus, the increase in polarization ratio is larger for the former sample than for the latter sample. In the future, more detailed study will be performed to quantify the strain relaxation and understand the origin of the reduction in the energy depth of localized states.

TABLE I. The fitted activation energy (E_a) for PL quenching for all as-grown and nonorod samples.

In composition	0.09	0.14	0.24	0.30
E_a (meV) as-grown	89	95	110	85
E_a (meV) nanorod	83	91	94	78

IV. CONCLUSION

In summary, *a*-plane GaN nanorod arrays with embedded $In_xGa_{1-x}N/GaN$ MQWs (x=0.09, 0.14, 0.24, and 0.30) by self-assembled Ni clusters and RIE-ICP dry etching have been fabricated successfully and their optical properties were studied in this work. The polarization-dependent PL reveals that the polarization ratio decreases slightly by 11% and 7% in the nanorod samples with x=0.09 and 0.14, respectively, while increases significantly by 79% and 27% in the nanorod samples with x=0.24 and 0.30, respectively. Moreover, from temperature-dependent PL results, low-(P_L) and high-energy (P_H) PL peaks, related to localized states and QWs, respectively, can be observed at low temperature after nanorod fabrication, which is similar to the as-grown samples. However, the intensity ratio of P_L and P_H decreases by 35%, 60%, 65%, and 49% for nanorod samples with increasing x from 0.09 to 0.30, respectively, indicating the reduction in localized states. This argument is verified from the smaller activation energies for PL quenching in the nanorod samples. In addition, multiple scattering along with strain relaxation is expected in these *a*-plane nanorod samples. Therefore, the variations in the polarization ratio mentioned above may be attributed to the competition between the polarization ratio reduction and enhancement effect by the multiple scattering along with strain relaxation and the reduction in localized centers, respectively. These results suggest that the nanorod fabrication can be an effective way to fabricate long-wavelength GaN-based LEDs with higher polarization ratio.

ACKNOWLEDGMENTS

These works were supported by the MOE ATU program and in part by the National Science Council of Republic of China (ROC) in Taiwan under Contract Nos. NSC-98-3114-M-009-001 and NSC-96-2221-E-009-094-MY3.

[1] S. Nakamura, M. Senoh, S. Nagahama, N. Iwasa, T. Yamada, T. Matsushita, H. Kiyoku, and Y. Sugimoto, Jpn. J. Appl. Phys., Part 2 **35**, L74 (1996).
[2] W. H. Sun, J. W. Yang, C. Q. Chen, J. P. Zhang, M. E. Gaevski, E. Kuokstis, V. Adivarahan, H. M. Wang, Z. Gong, M. Su, and M. A. Kahn, Appl. Phys. Lett. **83**, 2599 (2003).
[3] B. A. Haskell, F. Wu, M. D. Craven, S. Matsuda, P. T. Fini, T. Fujii, K. Fujito, S. P. DenBaars, J. S. Speck, and S. Nakamura, Appl. Phys. Lett. **83**, 644 (2003).
[4] A. Chakraborty, S. Keller, C. Meier, B. A. Haskell, S. Keller, P. Waltereit, S. P. DenBaars, S. Nakamura, J. S. Speck, and U. K. Mishra, Appl. Phys. Lett. **86**, 031901 (2005).
[5] A. Chitnis, C. Chen, V. Adivarahan, M. Shatalov, E. Kuokstic, V. Mandavilli, J. Yang, and M. A. Khan, Appl. Phys. Lett. **84**, 3663 (2004).
[6] P. Waltereit, O. Brandt, A. Trampert, H. T. Grahn, J. Menniger, M. Ramsteiner, M. Reiche, and K. H. Ploog, Nature (London) **406**, 865 (2000).
[7] S. Ghosh, P. Waltereit, O. Brandt, H. T. Grahn, and K. H. Ploog, Phys. Rev. B **65**, 075202 (2002).
[8] H. Masui, H. Yamada, K. Iso, J. S. Speck, S. Nakamura, and S. P. DenBaars, J. Soc. Inf. Disp. **16**, 571 (2008).
[9] H.-H. Huang and Y.-R. Wu, J. Appl. Phys. **106**, 023106 (2009).
[10] M. D. McCluskey, L. T. Romano, B. S. Krusor, D. P. Bour, N. M.

[This article is copyrighted as indicated in the article. Reuse of AIP content is subject to the terms at: http://scitation.aip.org/termsconditions. Downloaded to] IP: 140.113.38.11 On: Wed, 30 Apr 2014 10:00:39

Johnson, and S. Brennan, Appl. Phys. Lett. **72**, 1730 (1998).
[11]N. A. Ei-Masry, E. L. Piner, S. X. Liu, and S. M. Bediar, Appl. Phys. Lett. **72**, 40 (1998).
[12]T. Koyama, T. Onuma, H. Masui, A. Chakraborty, B. A. Haskell, S. Keller, U. K. Mishra, J. S. Speck, S. Nakamura, S. P. DenBaars, and T. Sota, Appl. Phys. Lett. **89**, 091906 (2006).
[13]C. H. Chiu, S. Y. Kuo, M. H. Lo, C. C. Ke, T. C. Wang, Y. T. Lee, H. C. Kuo, T. C. Lu, and S. C. Wang, J. Appl. Phys. **105**, 063105 (2009).
[14]T. S. Ko, T. C. Wang, R. C. Gao, H. G. Chen, G. S. Huang, T. C. Lu, H. C. Kuo, and S. C. Wang, J. Cryst. Growth **300**, 308 (2007).
[15]C. H. Chiu, M. H. Lo, C. F. Lai, T. C. Lu, H. W. Huang, Y. A. Chang, T. H. Hsueh, C. C. Yu, H. C. Kuo, S. C. Wang, C. F. Lin, and Y. K. Kuo, Nanotechnology **18**, 335706 (2007).
[16]Y. R. Wu, C. H. Chiu, C. Y. Chang, P. C. Yu, and H. C. Kuo, IEEE J. Sel. Top. Quantum Electron. **15**, 1226 (2009).
[17]B. Liu, R. Zhang, Z. L. Xie, J. Y. Kong, J. Yao, Q. J. Liu, Z. Zhang, D. Y. Fu, X. Q. Xiu, P. Chen, P. Han, Y. Shi, Y. D. Zheng, S. M. Zhou, and G. Edwards, Appl. Phys. Lett. **92**, 261906 (2008).
[18]D. Fu, R. Zhang, B. Wang, Z. Zhang, B. Liu, Z. Xie, X. Q. Xiu, H. Lu, Y. D. Zheng, and G. Edwards, J. Appl. Phys. **106**, 023714 (2009).
[19]E. Iliopoulos, D. Doppalapudi, H. M. Ng, and T. D. Moustakas, Appl. Phys. Lett. **73**, 375 (1998).
[20]J. Wu, W. Walukiewicz, S. X. Li, R. Armitage, J. C. Ho, E. R. Weber, E. E. Haller, H. Lu, W. J. Schaff, A. Barcz, and R. Jakiela, Appl. Phys. Lett. **84**, 2805 (2004).
[21]L. C. Chen and Y. L. Huang, Solid-State Electron. **48**, 1239 (2004).
[22]C. H. Chiu, T. C. Lu, H. W. Huang, C. F. Lai, C. C. Kao, J. T. Chu, C. C. Yu, H. C. Kuo, S. C. Wang, C. F. Lin, and T. H. Hsueh, Nanotechnology **18**, 445201 (2007).
[23]M. Leroux, N. Grandjean, B. Beaumont, G. Nataf, F. Semond, J. Massies, and P. Gibart, J. Appl. Phys. **86**, 3721 (1999).

[This article is copyrighted as indicated in the article. Reuse of AIP content is subject to the terms at: http://scitation.aip.org/termsconditions. Downloaded to] IP: 140.113.38.11 On: Wed, 30 Apr 2014 10:00:39